Environmental Science Nano

Accepted Manuscript

This article can be cited before page numbers have been issued, to do this please use: C. C. Parenti, S. Magni, A. Ghilardi, G. Caorsi, C. Della Torre, L. Del Giacco and A. Binelli, *Environ. Sci.: Nano*, 2020, DOI: 10.1039/D0EN00961J.

ROYAL SOCIETY OF CHEMISTRY

rsc.li/es-nano

View Article Online
DOI: 10.1039/D0EN00961J

Environmental significance

The physicochemical properties of nanoplastics (NPs) make them very suitable for the transfer of chemical contaminants, potentially enhancing their risk for the aquatic organisms. Nevertheless, few controversial evidences exist relied on the toxic effects caused by NP adsorption of environmental pollutants. To the best of our knowledge, this is the first study assessing the capability of polystyrene nanoparticles to adsorb triclosan (TCS), a known toxic chemical compound, and investigating the effect of the NP-TCS complex and each individual contaminant on a freshwater model. The results pointed out a clear shift in the toxicity when chemical and physical pollutants are bound together, rather than a simple additive, synergistic or competitive effect, suggesting the need to employ more complex interpretative models.

Does triclosan adsorption on polystyrene nanoplastics modify the toxicity of single contaminants?

Parenti[1], C.C., Magni[1], S., Ghilardi[1], A., Caorsi[1], G., Della Torre[1], C., Del Giacco[1], L., Binelli[1*], A.

[1]Department of Biosciences, University of Milan, Via Celoria 26, 20133 Milan, Italy

*Corresponding author e-mail: andrea.binelli@unimi.it

ABSTRACT

Physical and chemical properties of nanoplastics make them potential carriers for some environmental contaminants, modifying their biological effects. Nevertheless, the change in toxicity caused by pollutant adsorption on nanoplastics is still controversial, depending on the interactions between chemical and physical pollutants, the consequent change in bioavailability, the modification of intake, transport and accumulation in the organisms and also on the characteristics of contaminants. In this context, the aim of the present study was the evaluation of combined effects made by 0.5 µm nanobeads of polystyrene and triclosan adsorbed on their surface in comparison with those caused by the single contaminants. The systemic effects of 7-day exposure to nanoplastics, triclosan alone and to the nanoplastics-triclosan complex have been analyzed employing zebrafish larvae and using a multi-tier approach from the evaluation of cellular and molecular effects to the impact at organism level. Results highlighted as confocal microscopy evidenced nanobeads ingestion and translocation in several tissues and organs to guarantee the goodness of the exposure results. Behavioral assays were then conducted to highlight larval swimming defects as a 'real-time' readout of the potential effects on the whole organism, while a suite of several biomarkers and the functional proteomics were applied to investigate the effects at both cellular and molecular levels.

The whole dataset pointed out a clear modification in the toxicological effects of the nanoplastic-triclosan complex in comparison with single contaminants, proved by opposite behaviours in the larval swimming activity and modulation of diverse protein classes, as well as by different effects on

several biochemical endpoints. This means that the interaction between chemical and physical pollutants leads to more complicated responses than additive, synergistic or antagonist models, resulting in a modification of toxicity instead of its increase or decrease.

1. INTRODUCTION

Plastic invention surely represented one of the major technological innovations that changed our lifestyle and improved our wellness. Their versatile and unique characteristics (e.g. light weight, durability) allowed the application of plastic materials in several sectors, from the construction and transport industries to electrical and electronic applications, as well as the food conservation and healthcare. The incorrect disposal of plastic products is causing their increasing release in terrestrial and aquatic environments, since 79% of the plastic waste ever produced was accumulated in the natural environments or landfilled, while about 12% was incinerated and only 9% was recycled[1].

Once in the environment, larger plastic items can be fragmented into smaller debris by sunlight, mechanical abrasion, salinity and temperature variations[2]. These modifications can profoundly change plastic fate and toxicity, being more easily ingested and accumulated in the organisms. These smaller plastic pieces are called microplastics (MPs) and nanoplastics (NPs), which have been recently redefined as debris with a dimension between 1 μm to <1 mm and between 1 nm to <1 μm, respectively[3]. Due to their smaller dimension, these plastic debris represent the most dangerous fraction, since they can be potentially ingested by all aquatic and terrestrial organisms. Indeed, there are many evidences of the negative effects caused by MPs and NPs at various levels of the biological organization[4-10]. The next challenge is represented by the joined effects due to the interaction between MPs, NPs and chemical pollutants present in the environment, which can be adsorbed on the surface of plastic debris. Indeed, their high surface/volume ratio increases the sorption of other contaminants present in the surrounding matrix, making MPs and NPs suitable as physical carriers for these pollutants through all the environmental compartments, biota included. Having similar properties than natural suspended organic matter, MPs and NPs have a higher sorption capability for

hydrophobic contaminants, such as polychlorinated biphenyls (PCBs), polycyclic aromatic hydrocarbons (PAHs) and other benzene-ring derivatives[11]. Many studies demonstrated the capability of MPs and NPs to be a carrier also for some hydrophilic pollutants, due to the generation of oxidative groups during the plastic debris weathering that increase their polarity, roughness and porosity[12,13], as demonstrated for the adsorption on some MPs of perfluoro-octane-sulfonate (PFOS) and perfluoro-octane-sulfonamide (PFOA)[14], as well as of many antibiotics[15,16]. This means that smaller plastic debris can modify the overall bioavailability of the environmental contaminants for the organisms, magnifying or even decreasing the toxicity of pollutants bound together, as a consequence of the possible different relations in the ternary system chemical-plastic-organism[17].

In this context, the aim of our study was the evaluation of the possible change in toxicity after the adsorption of triclosan (TCS) onto 0.5 μm PS NPs (PNPs) in comparison with the effects evaluated after the exposures to single contaminants, by using zebrafish (*Danio rerio*) larvae as aquatic model organism. TCS is one of the current most investigated environmental pollutants due to its wide use in many consumer products (soaps, toothpastes, deodorants, textiles, shoes, toys, cosmetics) and the increasing evidences of its negative effects on the health of organisms, including humans. Being a hydrophobic chemical (log K_{ow}=4.76), TCS is a persistent environmental pollutant still present in natural environments in a concentration up to 5.2 μg L^{-1} in surface waters worldwide[18]. From the (eco)toxicological point of view, TCS and its by-products were reported to be endocrine disruptors in several model organisms, to affect immune responses, reactive oxygen species (ROS) production and also cardiovascular functions[19]. The ubiquitous presence of TCS in all the aquatic ecosystems worldwide makes this lipophilic contaminant prone to be transported by MPs and NPs, changing not only its environmental fate, but also the intake, accumulation and probably toxicity towards organisms.

Since the possible interaction between MPs, NPs and environmental contaminants has been conducted up to now using only the chemicals described above, our study represents a novelty for TCS, whose adsorption to plastic debris (polyethylene) has already been detected by Wu et al.[20].

Our experimental design comprised three different steps: 1) we firstly planned the sample preparation in order to eliminate the interference caused by TCS and PNPs freely present in the water when in co-exposure, through a preliminarily adsorption of environmental concentration of TCS (0.6 μg L^{-1}) onto PNPs (200 μg L^{-1}); 2) we then evaluate the ingestion, uptake and accumulation of virgin and doped PNPs in tissues and organs of zebrafish larvae by confocal microscopy; 3) lastly, we exposed zebrafish larvae to PNPs and TCS administered alone and to PNPs-TCS complex for 7 days, measuring many endpoints belonging to different levels of the biological organization. The multi-tier approach was based on the evaluation of possible alteration in swimming behavior, as the endpoint to assess the pollutants effects at a whole organism level, while a biomarker suite and functional proteomics were carried out to investigate the effects at cellular and molecular levels.

To the best of our knowledge, this is the first multidisciplinary study aimed to assess the potential of NPs to be a carrier for this antibacterial chemical, evaluating at the same time the possible change in toxicity, since there is only the study by Syberg et al.[21] describing the combined effect of TCS and polyethylene microbeads mixture administered to the marine copepod *Acartia tonsa*, based however only on the mortality as measured endpoint.

2. EXPERIMENTAL

2.1 *PNP characterization*

PNPs within the nanosized range of 0.4-0.6 μm (10% *w/v*) and fluorescent pink PNPs (1% *w/v*) with a comparable size (0.5 μm) were purchased from Spherotech Inc. (Lake Forest, IL, USA). Fluorescent nanobeads were only administered to larvae designed for confocal microscopy observations. Detailed information about PNPs characterization (size distribution, Z-potential, excitation and emission spectra) are shown in the Supplementary Materials (Tab. S1 and Fig. S1). Both PNP stock solutions contained sodium azide (0.02%) to prevent bacterial growth, which concentration decreased to 0.00001% in the working solution used for the exposure assays. Anyway, we previously certified that this very low concentration of bacteriostatic additive did not affect the investigated endpoints[9].

View Article Online
DOI: 10.1039/D0EN00961J

2.2 *TCS adsorption on PNPs and selection of concentrations*

Before the exposures, both the *non*-fluorescent and fluorescent PNPs were doped with TCS to obtain the TCS-contaminated plastic suspensions, thus creating a PNP-TCS single complex which was then administered to zebrafish larvae. This experimental plan allowed the elimination from the PNP-TCS exposure solution of the two interfering fractions constituted by the TCS and PNPs alone.

TCS contamination was performed adding PNPs (25 mg) and TCS (250 µg) in 3 glass bottles with 50 mL of deionized water and kept in constant mixing by a stirrer at 4 °C for 3 days in the dark. Then, the PNPs-TCS suspension was centrifuged for 15 min at 3,000 *g* at 25 °C to precipitate the nanobeads. The supernatants were collected and used to evaluate the fraction of TCS not adsorbed on the PNPs, while the pellets containing the doped PNPs were gently dried under nitrogen flow and maintained in glass vials until the exposure assays.

In order to check the fraction of TCS adsorbed on PNPs, each pellet was resuspended in methanol and the suspension was ultrasonicated for 30 min to re-separate the adsorbed TCS from the PNPs. The solution was then filtered (mesh=0.2 µm) to completely remove the remaining suspended PNPs. This solution, containing the TCS re-separated from PNPs, and the supernatants previously sampled, were analyzed by a liquid-liquid extraction (isooctane/methanol 4:1 *v/v* and hexane/water 2:1 *v/v*, respectively) followed by a gas-chromatographic analysis (TRACE GC coupled with a PolarisQ Ion Trap mass spectrometer, Thermo-Electron, Texas, USA). We calculated a concentration of 82 µg L^{-1} of TCS in the final solution, which was equal to the 36% of the initial concentration (250 µg L^{-1}), representing the percentage of TCS adsorbed on PNPs. Therefore, to remain within the environmental concentrations of this chemical, the PNP amount for the exposure was set to 200 µg L^{-1}, following the calculation showed in Tab. 1. This concentration corresponded to 0.6 µg L^{-1} of adsorbed TCS. Consequently, the same TCS concentration was used when the chemical was administered alone to zebrafish larvae.

View Article Online
DOI: 10.1039/D0EN00961J

2.3 *Exposure of zebrafish larvae*

AB strain adult zebrafish were reared in the facility at the Department of Biosciences, University of Milan, following the Italian laws, rules and regulations (Legislative Decree No. 116/92). According with the Italian Legislative Decree 26/2014, the project was carried out under the authorization of the Italian Ministry of Health (Aut. Min. No. 6/2019-PR).

We performed three independent experiments using different clutches of larvae from different fish to increase biological variability. Zebrafish larvae were exposed for 7 days, starting from the age of 4 days post fertilization (*dpf*) inside 800 mL glass beakers (approximately 100 larvae in 500 mL of zebrafish water in each beaker) and maintained at 28 °C on a 14h light:10h dark cycle. The exposures were carried out in semi-static conditions, changing the medium every 24 h and maintaining the water in constant mixing. Larvae were fed with commercially artificial diets (particle size < 100 μm) from 6 *dpf*. Control larvae (CTRL) were maintained in fish water (0.1 g L^{-1} Instant Ocean, 0.1 g L^{-1} $NaHCO_3$, 0.2 g L^{-1} $CaSO_4$ in deionized water with 0.1% methylene blue), while the three treatments consisted of: i) 0.6 μg L^{-1} TCS in zebrafish water, ii) 200 μg L^{-1} PNPs (corresponding to about $3x10^9$ nanobeads L^{-1}), and iii) 200 μg L^{-1} of the complex PNP-TCS.

At the end of exposures, larvae were sacrificed in tricaine (300 mg L^{-1}) and immediately processed for the following microscopy observations, genotoxicity assessments and behavioral test, or stored at -80 °C for further biomarker and proteomic analyses.

In the meantime, PNP-TCS suspensions and TCS solutions collected after 24 h in the exposure beakers were collected and analyzed in order to check for any TCS release from the particles, as well as the eventual reduction in TCS concentration after 24 h of exposure. We used the same method applied for the quantification of TCS adsorption (liquid-liquid extraction in hexane/water 2:1 *v/v* followed by a gas-chromatographic analysis).

View Article Online
DOI: 10.1039/D0EN00961J

2.4 *Confocal microscopy*

The ingestion and the accumulation of fluorescent PNPs (alone and combined with TCS) in zebrafish larvae were investigated by confocal microscopy technique. At the end of exposures, 20 larvae for each independent experiment were sacrificed as described above and fixed in paraformaldehyde (4% in PBS), then stored at 4 °C. Larvae selected for whole-mount observations were treated with protease K (P2308, Sigma Aldrich), stained with DAPI (4',6-diamidino-2-phenylindole) and directly mounted on microscope slides, while larvae designed for cryo-sectioning were washed in PBS (0.1 M) and sucrose (15% and 30%), included in the mounting medium (Bio Optica), frozen in dry ice and stored at -80 °C. Longitudinal and transversal sections (15 μm) were prepared using the cryostat CM 1850 (Leica, Wetzlar, Germania) at -20 °C. Cell nuclei were stained with DAPI.

For each experimental group (CTRL, PNP and PNP-TCS) we observed 10 whole-mount larvae and 10 slides of larval sections by a confocal microscope (Laser Scanning Confocal Microscope Nikon A1) to localize the internalized fluorescent PNPs in the exposed organisms. The assessment of the orthogonal projections of Z-stacks pictures guaranteed that PNPs were effectively inside the tissues and not a simple artefact due to the transport made by the blade of the cryostat.

2.5 *Larval swimming activity*

Potential behavioral alterations induced by the three different treatments were evaluated on 12 larvae for each experimental group (36 total larvae for each treatment), using the DanioVision™ tracking system (Noldus IT, Wageningen, Netherlands).

Each larva was put in a single well of a 24-multiwell plate and submitted to an alternating dark/light test based on 10 minutes of adaptation, followed by 2 cycles of 20 min of dark and 10 min of light[9], recording their swimming activity at 30 frames/s. During the entire test, temperature was maintained at 28 °C by the DanioVision Temperature Control Unit.

Acquired data were analyzed by the software EthoVision XT (Noldus IT, Wageningen, Netherlands), measuring the following parameters: total distance moved (mm), turn angle (degree) and thigmotaxis

(wall-hugging behavior). The software was also applied to create and visualize graphical representations of larval swimming activity, such as tracks (Fig. S3A) and heatmaps (Fig. S3B), where different colors represented the frequency of a specific position (hotspots) in the well.

2.6 *Biomarker*

Biomarker methods are thoroughly described in Supplementary Materials. Briefly, cell viability was assessed by the trypan blue dye exclusion method before the genetic damage tests to guarantee a viability higher than 80%[22]. Genotoxicity assessments were performed according to Parolini et al.[23] by using pools of 7 larvae for each experimental group (3 pools of 7 individuals for each treatment). Genotoxicity was evaluated measuring the frequency of apoptotic and necrotic cells, as well as micronuclei (MN) which pointed out fixed and irreversible DNA damage.

The effects on detoxification systems was assessed by ethoxyresorufin-O-deethylase (EROD) and glutathione S-transferase (GST) activities, while the oxidative stress level was evaluated by superoxide dismutase (SOD), catalase (CAT) and glutathione peroxidase (GPx) activities, and by the measurement of reactive oxygen species (ROS) production on pools of 35 larvae from each experimental group (3 pools of 35 individuals for each treatment).

Lastly, the presence of neurotoxic effects was assessed by the level of acetylcholinesterase (AChE) activity, using the 5,5'-dithiobis-2-nitrobenzoic acid (DTNB) as reagent[7]. Due to the strong connection between neuronal alterations and behavior, for this test we pooled together larvae previously tested for behavioral changes (36 total larvae for each treatment).

All data resulting from enzymatic analyses and ROS evaluation were normalized on the protein total content of each sample measured by the Bradford method[24].

2.7 *Functional proteomics*

The modulation of protein expression in control and treated larvae was investigated by the *gel-free* proteomic technique[8]. At the end of the exposure, pools of 20 larvae for each experimental group (3

pools of 20 individuals for each treatment) were homogenized in 300 µL of lysis buffer (described in Supplementary Materials). Proteins were precipitated, reduced, alkylated and then digested adding trypsin. Peptides were then purified by reverse phase chromatography, using Zip Tips (µ-C18; Millipore, Milan, Italy)[8] and analyzed with a mass spectrometer as reported by Magni et al.[8] with some modifications (described in Supplementary Materials).

2.8 *Statistical analysis*

Statistical analyses on behavior and biomarker data were performed using STATISTICA 7.0 software. After having checked the normality and homoscedasticity of biomarker data, the significance was evaluated by one-way analysis of variance (ANOVA) followed by the Duncan's Multiple Range *post-hoc* test (DMRT), taking $p<0.05$ as significance cut-off. Regarding the proteomic results, a Student t-test was performed between control and treated.

3. RESULTS

3.1 *Check of the experimental conditions*

The check of the possible release of TCS from the doped PNP by gas chromatographic analyses showed the complete absence of the chemical in the exposure beakers after 24 h of exposure, pointing out that TCS did not detach from the particles. This means as the ecotoxicological effects due to the TCS-PNP complex presented below are certainly due to the combination of the two contaminants because our experimental design was able to eliminate the interference due to TCS and PNP present alone in the exposure suspensions. Furthermore, the analyses of TCS concentration in the exposure solutions after 24 h revealed a decrease of about 30% (0.4 µg/L) in the beakers containing 0.6 µg/L of TCS alone, confirming the need to perform the exposures in semi-static conditions by a daily renewal of chemical.

View Article Online
DOI: 10.1039/D0EN00961J

3.2 *PNP uptake and accumulation in zebrafish larvae*

Whole mount observations by confocal microscope confirmed the PNP uptake by larvae, both for virgin PNPs and PNP-TCS complex (Fig. 1). On the other hand, the capability of PNPs to pass biological membranes and accumulate in different tissues was already demonstrated also for zebrafish embryos[9]. Nevertheless, new findings have emerged from larval section observations, since we visualized PNPs both in the eye (Fig. 2) and in the trunk (Fig. 3). Furthermore, we did not observe any differences in the amount of ingested PNPs between virgin ones and PNP-TCS complex, suggesting that TCS adsorption did not modify the particles intake.

3.3 *Effects at individual level*

At the end of exposures, the effects of the three treatments on fish behavior were evaluated by measuring their swimming activity. Results highlighted an opposite effect of TCS when administered alone or combined with PNPs. Indeed, we observed both a hypo- and a hyper-activity of zebrafish larvae compared to controls, respectively (Fig. 4A). In detail, the variation was significant both for the dark ($F_{3,156}$=21.28 and $p<0.001$) and the light phase ($F_{3,74}$=50.15 and $p<0.001$; Fig. 4B). By contrast, PNPs administered alone did not significantly affect the total distance travelled by larvae. Regarding the other considered parameters, such as turn angle (Fig. S2A) and thigmotaxis (Fig. S2B), no significant differences were observed upon all exposure conditions.

3.4 *Effects at sub-organism level*

Biomarker analyses pointed out significant variations of MN frequency ($F_{3,20}$=4.92 and $p<0.05$), as well as GST ($F_{3,19}$=5.75 and $p<0.01$) and GPx activities ($F_{3,20}$=3.64 and $p<0.05$) (Fig. 5). In detail, we observed a significant increase ($p<0.01$) of MN frequency due to TCS administered alone, compared to controls, while a significant decrease was found in PNP ($p<0.05$) and PNP-TCS ($p<0.05$), compared to TCS. Regarding oxidative endpoints, a significant increase of GST and GPx activity was detected in organisms exposed to TCS, compared to controls ($p<0.01$ and $p<0.05$,

respectively). The measured activities of these enzymes were also significantly different between PNP-treated groups and TCS-treated group. In detail, GST activity decreased in PNPs and PNP-TCS, compared to TCS ($p<0.01$ and $p<0.05$, respectively), while GPx activity decreased in PNP-TCS, compared to TCS ($p<0.05$). Lastly, any significant effects of PNPs, both virgin and contaminated, were pointed out by biomarker analyses.

3.5 *Effects on proteome*

We identified 1807 proteins, 1480 of which were subsequently quantified. More in detail, PNPs modified 43 proteins, 8 of which were significantly different ($p<0.05$) from controls, but not above the 2-fold change threshold (Fig. S4A). The remaining 35 proteins were quite equally divided between up-regulated (16) and down-regulated (19) proteins (Fig. 6A).

TCS was able to modulate 68 different proteins, 45 of which were significantly different ($p<0.05$) to controls, but not above the 2-fold change threshold (Fig. S4B). Then, we found 10 proteins up-regulated and 13 down-regulated (Fig. 6A).

The PNP-TCS complex modified a total of 29 proteins, all above the significance and the biological effect threshold of the 2-fold change (Fig. S4C). In particular, we measured 11 up-regulated and 18 down-regulated proteins (Fig. 6A).

The entire proteomic dataset revealed a number of proteins modulated by PNPs (35) higher than those changed by PNP-TCS complex (29) and TCS (23), with different biological functions: PNPs mainly modified proteins involved in genetic processes, which represent the 25% of the total changed proteins, followed by cytoskeleton (22%), energy (17%) and catalytic activity (11%). Calcium metabolism and transport counted for 8%, while proteins involved in the immune system were only 3%. Six % of all the misregulated proteins do not have known function (Fig. 7A).

More than a quarter of proteins modulated by TCS belongs to energy group (26%), followed by genetic processes (22%) and catalytic activities (18%), while cytoskeleton dropped to 13% only (Fig.

7B). The remaining 17% included proteins entangled in transport, development and immune system, while 4% of identified proteins have no known annotated function.

The PNP-TCS complex modulated many proteins unrelated neither to PNPs nor TCS. The cytoskeleton proteins were the most affected by the complex (35%), while the second most modified group (genetic processes) accounted for 17% of the changed proteins (Fig. 7C). Catalytic activity (14%) and energy (10%) were less represented than in the other treatments, while modifications of structural proteins (7%) appeared.

The Venn diagram (Fig. 6B) confirmed the different effects due to pollutants, since only 7 proteins were in common among the three treatments (Tab. S2), highlighting the lack of similar effects on common biological pathways. This is expected for the physical and chemical pollutants, with different routes of intake, accumulation and mechanism of actions (MoAs), as confirmed by the only 3 proteins in common between these treatments (Fig. 6B). The MoA of the PNP-TCS complex seemed to be more similar to PNPs than TCS, as indicated by the 8 different proteins in common between the two treatments *versus* the only 4 changed proteins in common between TCS and PNP-TCS complex (Fig. 6B).

4. DISCUSSION

The aim of this study is a novelty in the NP scenario since we investigated both the role played by NPs as vector for TCS and the possible ecotoxicological consequences of the intake of the PNP-TCS complex in relation to the administration of the two single pollutants.

4.1 *TCS adsorption and microscopy observations*

The first step to certify the following ecotoxicological results was the confirmation of the adsorption of TCS onto PNPs and the intake of PNPs and the complex in the biological model.

The high amount of TCS adsorbed on PNPs, corresponding to 36% of the starting TCS concentration added in the suspension, confirmed the high sorption capability of PS for hydrophobic contaminants.

This is due to the presence of several benzene rings in its polymeric structure, which increase the distance between the chains, thus facilitating the contaminant attachment and integration[25]. On the other hand, the sorption behavior of TCS for PS was well described by Li et al.[26], who showed that the proportion of the adsorbed TCS increase with decreasing PS particles size.

The smaller size of NPs not only increases their sorption capability, but also enhances their ability to bioaccumulate contaminants inside organism tissues[27]. Our study confirmed this behavior since we observed the presence of PNPs into the gastrointestinal tract of zebrafish larvae, yet an external compartment, but also discovered that some PNPs, both pristine and contaminated by TCS, were distributed in other organs, such as the eye (Fig. 2) and in the trunk (Fig. 3).

The role played by NPs as carrier for some environmental contaminants was already noticed in a study performed on adult zebrafish exposed to NPs (1 mg L^{-1}), bisphenol A (BPA; 1 µg L^{-1}) and their mixture, that showed the presence of both contaminants in viscera, gills, head and muscles, leading also to a higher BPA accumulation in the brain, which was related to a dopaminergic neurotoxic effect[28]. Furthermore, an increased bioaccumulation of phenanthrene (0.1 mg L^{-1}) was observed in *Daphnia magna* when co-exposed to NPs (5 mg L^{-1}) for 14 days, highlighting their action as vectors of PAHs[29].

4.2 *Effects at organism level*

It has been observed that zebrafish larvae, when exposed only to an alternating light/dark period, showed a pattern of increased movement in the dark phase, probably due to decreased predator threat, followed by a resting state in the light phase[30]. Thus, the possible alteration of this natural behavior has been used to assess the effects of any substance that might be able to generate neurotoxic effects, such as drugs, metals and nanoparticles[31].

We applied this concept to our experiments, in which both TCS and PNP-TCS complex significantly affected larval swimming activity, as opposed to PNPs administered alone (Fig. 4). Interestingly, we observed that TCS and PNP-TCS complex had an opposite effect on larval swimming since the total

distance moved significantly decreased during both dark and light phases in the larvae exposed to TCS, while it increased for those exposed to the PNP-TCS complex.

The alteration of locomotor behavior of zebrafish larvae caused by the exposure to environmental contaminants have been already observed. For instance, polybrominated diphenyl ethers (PBDEs) and their metabolites caused an altered swimming behavior, showing both an increased and decreased locomotion, depending on the molecules, concentrations and exposure conditions[32,33]. The evidence that diverse treatments can differently affect movements was also reported in the study by Ali et al.[34], in which zebrafish embryos were exposed to a wide range of toxic compounds with different MoAs. In our study, the TCS exposure induced significant larval hypoactivity, which could be attributable to affected locomotor system development[35], while the hyperactivity observed in larvae exposed to the PNP-TCS complex could be attributed to visual defects[35] and/or an increased stress/anxiety level[36].

Although these hypotheses should be in deep investigated since the differences in behavioral patterns strictly depend on the neuronal targets of tested contaminants[37], some results from the proteomic approach seemed to explain the opposite swimming behaviour noticed after the TCS and PNP-TCS complex treatments, as shown below. Moreover, we might suggest that the opposite effect of TCS and PNP-TCS complex can be attributable to the accumulation of the chemical in different body districts. Indeed, when TCS is administered alone, being a lipophilic compound, it bioaccumulates in lipid tissues, such as yolk, but when adsorbed to PNPs, it is forced to follow the physical pollutant that accumulate in other tissues and organs, modifying its MoA against different cellular pathways, as previously demonstrated in our study[38]. This could not be confirmed in our experiments due to the small size of the zebrafish larvae. Another possible hypothesis could be related to the metabolization of TCS by the CYP 450 detoxification system, mainly present in liver, producing the more toxic metabolite methyl-TCS[39]. Thus, the PNP-TCS complex might modify the accumulation pathway, eliminating or simply decreasing the amount of TCS that ends in the liver and, consequently, reducing the methyl-TCS production and changing its (eco)toxicological effects.

View Article Online
DOI: 10.1039/D0EN00961J

4.3 *Effects at sub-organism level*

The evaluation of sub-individual effects on exposed organisms was performed to further understand the different toxicity behavior observed between TCS, PNPs and PNP-TCS complex. The biomarker approach did not show any significant effect of the PNP treatment, both pristine and contaminated, pointing out only few effects for TCS administered alone. On the other hand, our results are comparable to those shown in a recent study, in which the evaluation of biomarker responses was applied to test the effects of pristine PE fragments on zebrafish larvae, showing the lack of alteration on both the oxidative stress and AChE activity[40]. However, reported effects of NPs on aquatic organisms are varied and sometimes controversial, depending on particles concentration, physical and chemical properties, and composition[41]. Moreover, our data represent the first evidence concerning the effects of TCS-contaminated NPs on zebrafish, making it difficult to directly compare our results to those from other studies. The only existing studies reported an increased toxicity of NPs when combined with phenanthrene in *Daphnia magna*[29], and Chen et al.[28] pointed out that a mixture of NPs and BPA led to an increase of neurotoxic effects in zebrafish, compared to NPs and BPA alone.

Our results did not highlight any effects on AChE activity (Fig. 5), but the measurement of this unique endpoint is not sufficient to identify possible neurotoxic effects in zebrafish cholinergic system, as also reported by Chen et al.[28]. Thus, further analyses are needed to exclude the presence of neurological damages which could have been responsible for the locomotion alterations we observed. Unlike PNPs, the slight and non-homogeneous effects caused by the TCS exposure on zebrafish larvae were only related to a significant ($p<0.05$) increase of GST, GPx and micronuclei formation (Fig. 5), confirming the results obtained in our previous study on zebrafish embryos in which we found that environmental concentrations of TCS (0.1-1 $\mu g\ L^{-1}$) were able to induce the activation of detoxification systems and generate cytotoxicity[42]. The lack of effects when TCS is bound to PNPs suggested a decrease of the toxicological profile of the complex that can be explained by two different hypotheses: 1) chemical was not desorbed from PNPs, making impossible exploiting its effect on the

selected endpoints; 2) the complex formation decreased the bioavailability of TCS, reducing its concentration in *D. rerio* larvae.

As final remark, the biomarker dataset gave another evidence about the modification of the ecotoxicological effects for the 3 different exposures and the extreme complexity of the relationship between physical and chemical pollutants, as well as the need to measure many different endpoints along the biological organization able to obtain a wider ecotoxicological picture.

4.4 *Effects on proteome*

The last step of the multi-tier approach was the proteomics, a high-throughput technology which complements existing techniques on revealing the MoA of toxic substances. We focused the discussion only on the changed proteins whose functions can be related to results revealed by the other two applied approaches, while the description of the other classes of modulated proteins is shown in the Supplementary Materials.

4.4.1 *Structural proteins*

Unlike the other two treatments, the PNP-TCS complex selectively modified two specific structural proteins (Fig. 6A), namely the Crystallin γ M2d2 (CryM2d2) and Collagen type XIV α1b (Col4α1b), confirming the zebrafish eye as a target for NPs, as also pointed out by microscopy (Fig. 2). This evidence is of particular interest as it may be closely related to the hyperactivity of zebrafish larvae observed after the exposure to PNP-TCS complex (Fig. 4) since visual defects have been identified precisely as one of the possible causes of behavioral changes[35].

CryM2d2 is a structural constituent of the vertebrate lens crystallin which is mainly composed by α-, β- and γ-crystallin proteins[43]. Although the γM-crystallin class represents more than 70% of the eye lens proteins in zebrafish[44], their functional role is not completely clear. Interestingly, Pande et al.[45] reported that γ-crystallins are essential for maintaining lens transparency since their aggregation decreases the lens homogeneity and lead to cataract. Thus, the over-production of CryM2d2 noticed

after the PNP-TCS complex exposure could be a signal of eye defects due to an increased crystallization of the γ-crystallins, whose deposits in the lens are typical in several non-genetic forms of cataract [46].

A different function is related to Col4α1b, the other structural protein modulated only by the PNP-TCS complex, whose change can be related to the eye functioning. Col4α1b belongs to the superfamily of fibril associated collagens with interrupted triple helices (FACIT)[47] which is present in some connective tissues, such as skin, tendon, and also cornea[48]. Its main function is the regulation of the formation and size of the collagens fibrils to guarantee the stability and integrity of the extracellular matrix and its fibrillar collagen network[49]. Young et al.[50] found that type XIV collagen is highly expressed in the early stage of development of chicken embryos and it is involved in the regulation of fibrillogenesis in the corneal stroma.

The clear evidence that the two structural proteins modulated exclusively by the PNP-TCS complex are directly related to the eye development and that they can be the possible reason of the hyperactivity noticed pointed out the need of future in-depth studies on the effect exerted by plastics and their adsorbed environmental pollutants in the early stages of eye development. This represents another proof about the change of the ecotoxicological behaviour when the two pollutants were administered bound together and probably due to the capability of PNPs to have the eye as carrier, but at the same time to exert these specific effects only when in combination with TCS. On the other hand, previous studies identified the eye as one of the preferential targets for NPs: van Pomeren et al.[51] demonstrated the deposit of 25 and 50 nm PNPs in the zebrafish eye and Lee et al.[52] observed the accumulation of 50 nm PNPs in the retina of zebrafish embryos at 24 hours post-fertilization (*hpf*).

4.4.2 *Proteins of energetic pathways*

This was the biggest group of proteins modulated by TCS (Fig. 7), suggesting a direct effect of the chemical on the energy stock and energetic pathways able to determine the hypo-activity observed after the behavioral tests (Fig. 4).

The KEGG (Kyoto Encyclopedia of Genes and Genomes) PATHWAY database highlighted that 4 proteins (Fructose-bisphosphate aldolase C-A, Aldoca; Glycogenin 1b, Gyg1b; Glutaryl-CoA dehydrogenase, Gcdhl; ATPase H^+-transporting V1, Atp6v1ab) out of 6 modulated by TCS were involved in some energetic pathways. In detail, Aldoca is directly involved in one of the essential sub-pathways of glycolysis that synthesizes D-glyceraldehyde 3-phosphate and glycerone phosphate from D-glucose. Since several previous studies on fish species[53-56] showed an upregulation of Aldoca during conditions reflecting a strong energy demand, the increased production of this glycolytic enzyme noticed in our experiments suggested the need of an energy over-production for zebrafish larvae, through the formation of glycolytic ATP molecules, probably to counteract the effects due to TCS. One of the possible effects of TCS could be thus related to a rise of energy demand and the subsequent decrease in the energy stock available to other activities. Therefore, the hypo-activity revealed after the TCS exposure (Fig. 4) can be an indirect consequence of this energy lowering. This hypothesis seemed to be also confirmed by the downregulation of Gyg1b (Fig. 6A) which is involved in the glycogen biosynthesis, fundamental as energetic reserve. Unfortunately, no previous studies are available for Gyg in *Danio rerio* but, from the ecotoxicological point of view, since the skeletal muscles use glycogen as the main source of energy for anaerobic metabolism to fuel short and intense activity, the downregulation of Gyg1b suggested once more a deficit in the energy storage at muscular level that could explain the movement decrease observed during the behavioral assays.

The functions of the other two proteins belonging to the energy group (Gcdhl and Atp6v1ab) that were downregulated by TCS also supported this hypothesis. Indeed, Gcdhl is a mitochondrial protein involved in the pathway of fatty acid degradation that catalyzes the transformation of Glutaryl-CoA into Crotonyl-CoA[57]. This is one of the final steps to produce acetyl-CoA, the entry molecule for the citric acid cycle that represents the main energy supply for animals. In humans, GCDH deficiency

creates a neurodegenerative disease (Glutaric aciduria Type 1) characterized by an irreversible dystonic-dyskinetic movement disorder due to the striatal neuronal death[58].

The Atp6v1ab, previously known as Atp6v1a, is indirectly related to glycolysis and pentose phosphate pathways being involved in ATP metabolic process and hydrogen ion trans-membrane transport. Besides representing a proton transporter for all the steps of the energy pathways, this protein is also involved in the crucial role of ammonia excretion in zebrafish larvae. Indeed, Shih et al.[59] demonstrated that the H^+-ATPase of the apical membrane of the pump-rich cells (HRCs) of the *Danio rerio* gills contribute for more than 70% to skin acid secretion and that the knockdown of the H^+-pump gene *atp6v1a* significantly decreased the NH_4^+ secretion.

4.4.3 *Cytoskeleton proteins*

Five out of the 8 modulated proteins in common between PNPs and PNP-TCS complex belong to cytoskeleton (myosin heavy polypeptide 1, skeleton muscle, Myhz1.1; myosin heavy polypeptide 2, fast muscle-specific, Myhz2; myosin heavy chain b, Myhb, slow myosin heavy chain 1, Smyhc1; plectin a, Pleca). These 5 up-regulated proteins are mainly related to the skeletal muscle system development and organization in zebrafish[60-63] (Tab. S2). Very interestingly, the KEEG PATHWAY Database revealed that three of them (Myhz2, Myhb and Smyhc1) are also functional elements of the paracellular tight junctions (TJs) of skeleton muscles, that connect the absorptive epithelial cells at the apical membrane in the gastrointestinal tract[64]. TJs are multiprotein complexes whose main function is to assemble a paracellular barrier, allowing a selective diffusion on the basis of size and charge of ions and molecules[65]. According to most recent data, ions and molecules are hypothesized to permeate through the TJs by two different routes: pore and leak pathways[66,67]. The first one is the preferential pathway for molecules smaller than 0.4 nm[68], while the leak pathway is a nonspecific way of entrance for macromolecules with a diameter up to 6 nm[69]. Although the PNPs administered to zebrafish in our study, with a size of 0.5 μm, should not enter through the TJs, they modified the amount of three of the structural proteins of this paracellular barrier which regulate actin in order to

control the cell polarity. Thus, the same co-regulation noticed both for PNP and PNP-TCS complex might point out a possible alteration in the intercellular defence mechanism related just to PNPs.

At a more general level of discussion, the great impact on cytoskeleton proteins highlighted for PNPs and PNP-TCS complex confirmed as the increase of oxidative stress is the main effect for these physical contaminants. Indeed, several studies have been shown that the proteins of cytoskeleton are one of the first targets of the oxidative stress[70-72], as also found in our previous study in which we administered two different mixtures of MPs to the freshwater bivalve *D. polymorpha*[8].

4.4.4 *Final remarks for proteomics*

Proteomics has proven to be a very useful and sensitive tool in the evaluation of the ecotoxicity due to NPs, whose infiltration in the organism tissues follows different pathways than chemicals, passing through the biological barriers and/or to exploit the transmembrane canals and TJs, depending on their size. The logical consequence is that the number of NPs that enters the organism tends to be lower than chemicals which simply follow a concentration gradient, constraining the use of very sensitive analytical methodologies to observe the presence of NPs in the tissues and also to evaluate their toxicological effects. The high-throughput technology based on proteomics is surely one of the possible solutions because of its sensitivity that allows the evaluation of the impact made on different cellular pathways and suggests possible MoAs, as demonstrated in this study. Indeed, proteomics confirmed that the combined effect of chemical and physical pollutants should be considered more as a modification of toxicological behavior rather than a mere increase or decrease in toxicity, since PNP-TCS complex modulated both proteins in common with TCS and PNPs, but it also changed several other proteins not modulated by the two contaminants administered alone. The most evident case is the one related to the two structural proteins upregulated by the PNP-TCS complex alone, thus suggesting a complementary effect on the early-stages of eye development only when the two contaminants were bound together.

Figure 8 summarizes the network of proteins related to the same biological function and the relative effect of the three different contaminants. This toxicological behavior explains exactly what has been previously said, namely that the PNP-TCS complex intrinsically possesses not only the capability to act both on proteins-target modulated by PNPs and TCS alone, but also to acquire new toxicological characteristics.

5. CONCLUSIONS

The purpose of this study was to open a new perspective on investigating the risk associated to the action of NPs as carrier of environmental pollutants. Overall, the whole dataset obtained with the multi-step approach made a clear response to the main goal of this study, since it highlighted as the formation of the PNP-TCS complex heavily modified the toxicological behaviour of the single contaminants. It almost seems that the bond between chemical and physical compounds creates a kind of new pollutant with emerging and unpredictable characteristics that are able to change the toxicological pathways and targets. From the ecotoxicological point of view, our multiple results highlighted how the PNP-TCS complex showed a change in toxicological behavior with respect to individual contaminants instead of a simple decrease or increase of toxicity, suggesting the need to go beyond classical models based on additive, synergistic or antagonist effects that regulate interactions between chemical pollutants.

Another crucial result obtained is related to the need for a multilevel approach that covers many steps of biological organization. Indeed, differences found in the responses clearly showed that its application is critical, especially in this kind of studies, in which the relation between chemical and physical compounds is unknow and drives to unpredictable effects.

6. CONFLICTS OF INTEREST

There are no conflicts to declare.

View Article Online
DOI: 10.1039/D0EN00961J

7. ETHICAL STATEMENT

All animal procedures were performed in accordance with the Guidelines for Care and Use of Laboratory Animals of the University of Milan and approved by the Animal Ethics Committee of the Italian Ministry of Health (Aut. Min. No. 6/2019-PR).

REFERENCES

1. R. Geyer, J. R. Jambeck and K. L. Law, Production, use, and fate of all plastics ever made, *Sci. Adv.*, 2017, **3**, e1700782.
2. T. O'Brine and R. C. Thompson, Degradation of plastic carrier bags in the marine environment, *Mar. Pollut. Bull.*, 2010, **60**, 2279-2283.
3. N. B. Hartmann, T. Huffer, R. C. Thompson, M. Hasselov, A. Verschoor, A. E. Daugaard, S. Rist, T. Karlsson, N. Brennholt, M. Cole, M. P. Herrling, M. C. Hess, N. P. Ivleva, A. L. Lusher and M. Wagner, Are we speaking the same language? Recommendations for a definition and categorization framework for plastic debris, *Environ. Sci. Technol.*, 2019, **53**, 1039-1047.
4. Lee 2013
5. Y. Lu, Y. Zhang, Y. Deng, W. Jiang, Y. Zhao, J. Geng, L. Ding and H. Ren, Uptake and accumulation of polystyrene microplastics in zebrafish (*Danio rerio*) and toxic effects in liver, *Environ. Sci. Technol.*, 2016, **50**, 4054.
6. L. Lei, S. Wu, S. Lu, M. Liu, Y. Song, Z. Fu, H. Shi, K. M. Raley-Susman and D. He, Microplastic particles cause intestinal damage and other adverse effects in zebrafish *Danio rerio* and nematode *Caenorhabditis elegans*, *Sci. Tot. Environ.*, 2018, **619-620**, 1-8.
7. S. Magni, F. Gagné, C. André, C. Della Torre, J. Auclair, H. Hanana, C. C. Parenti, F. Bonasoro and A. Binelli, Evaluation of uptake and chronic toxicity of virgin polystyrene microbeads in freshwater zebra mussel *Dreissena polymorpha* (Mollusca: Bivalvia), *Sci. Tot. Environ.*, 2018, **631-632**, 778-788.

8. S. Magni, C. Della Torre, G. Garrone, A. D'Amato, C. C. Parenti and A. Binelli, First evidence of protein modulation by polystyrene microplastics in a freshwater biological model, *Environ. Pollut.*, 2019, **250**, 407-415.

9. C. C. Parenti, A. Ghilardi, C. Della Torre, S. Magni, L. Del Giacco and A. Binelli, Evaluation of the infiltration of polystyrene nanobeads in zebrafish embryo tissues after short-term exposure and the related biochemical and behavioural effects, *Environ. Pollut.*, 2019, **254**, 112947.

10. M. S. S. Silva, M. Oliveira, D. Lopéz, M. Martins, E. Figueira and A. Pires, Do nanoplastics impact the ability of the polychaeta *Hediste diversicolor* to regenerate?, *Ecol. Indic.*, 2020, **110**, 105921.

11. X. Liu, J. Xu, Y. Zhao, H. Shi and C. H. Huang, Hydrophobic sorption behaviors of 17ß-Estradiol on environmental microplastics, *Chem.*, 2019, **226**, 726-735.

12. K. N. Fotopoulou and H. K. Karapanagioti, Surface properties of beached plastic pellets, *Mar. Environ. Res.*, 2012, **81**, 70-77.

13. F. Yu, C. Yang, Z. Zhu, X. Bai and J. Ma, Adsorption behavior of organic pollutants and metals on micro/nanoplastics in the aquatic environment, *Sci. Tot. Environ.*, 2019, **694**, 133643.

14. F. Wang, K. M. Shih and X. Y. Li, The partition behavior of perfluoro-octanesulfonate (PFOS) and perfluoro-octanesulfonamide (PFOA) on microplastics, *Chem.*, 2015, **119**, 841-847.

15. X. C. Shen, D. C. Li, X. F. Sima, H. Y. Cheng and H. Jiang, The effects of environmental conditions on the enrichment of antibiotics on microplastics in simulated natural water column, *Environ. Res.*, 2018, **166**, 377-383.

16. J. Li, K. Zhang and H. Zhang, Adsorption of antibiotics on microplastics, *Environ. Pollut.*, 2018, **237**, 460-467.

17. B. Nowack and T. D. Bucheli, Occurrence, behavior and effects of nanoparticles in the environment, *Environ. Pollut.*, 2007, **150**, 5-22.

18. S. Jagini, S. Konda, D. Bhagawan and V. Himabindu, Emerging contaminant (triclosan) identification and its treatment: A review, *SN Appl. Sci.*, 2019, **1**, 640.

19. L. M. Weatherly and J. A. Gosse, Triclosan exposure, transformation, and human health effects, *J. Toxicol. Environ. Health*, Part B, 2017, **20(8)**, 447-469.

20. C. Wu, K. Zhang, X. Huang and J. Liu, Sorption of pharmaceuticals and personal care products to polyethylene debris, *Environ. Sci. Pollut.*, 2016, **23**, 8819-8826.

21. K. Syberg, A. Nielsen, F. R Khan, G. T. Banta, A. Palmqvist and P. M. Jepsen, Microplastic potentiates triclosan toxicity to the marine copepod *Acartia tonsa* (Dana), *J. Toxicol. Environ. Health*, Part A, 2017, **80**, 23-24, 1369-1371.

22. R. R. Tice, E. Agurell, D. Anderson, B. Burlinson, A. Hartmann, H. Kobayashi, Y. Miyamae, E. Rojas and Y. Sasaki, Single cell gel/Comet assay: guidelines for in-vitro and in-vivo genetic toxicology testing, *Environ. Mol. Mutagen.*, 2000, **35**, 206-221.

23. M. Parolini, A. Ghilardi, C. Della Torre, S. Magni, L. Prosperi, M. Calvagno, L. Del Giacco and A. Binelli, Environmental concentrations of cocaine and its main metabolites modulated antioxidant response and caused cyto-genotoxic effects in zebrafish embryo cells, *Environ. Pollut.*, 2017, **226**, 504-514.

24. M. M. Bradford, A rapid and sensitive method for the quantification of microgram quantities of protein using the principle of protein-dye binding, *Anal. Biochem.*, 1976, **72**, 248-254.

25. O. S. Alimi, J. F. Budarz, L. M. Hernandez and N. Tufenkji, Microplastics and nanoplastics in aquatic environments: Aggregation, deposition, and enhanced contaminant transport, *Environ. Sci. Technol.*, 2018, **52**, 1704-1724.

26. Y. Li, M. Li, Z. Li, L. Yang and X. Liu, Effects of particle size and solution chemistry on triclosan sorption on polystyrene microplastic, *Chemosphere*, 2019, **213**, 308-314.

27. J. P. da Costa, P. S. M. Santos, A. C. Duarte and T. Rocha-Santos, T., (Nano)plastics in the environment - Sources, fates and effects, *Sci. Tot. Environ.*, 2016, **566-567**, 15-26.

28. Q. Chen, D. Yin, Y. Jia, S. Schiwy, J. Legradi, S. Yang and H. Hollert, Enhanced uptake of BPA in the presence of nanoplastics can lead to neurotoxic effects in adult zebrafish, *Sci. Total Environ.*, 2017, **609**, 1312-1321.

29. Y. Ma, A. Huang, S. Cao, F. Sun, L. Wang, H. Guo and R. Ji, Effects on nanoplastics and microplastics on toxicity, bioaccumulation, and environmental fate of phenanthrene in fresh water, *Environ. Pollut.*, 2016, **219**, 166-173.

30. R. C. MacPhail, J. Brooks, D. L. Hunter, B. Padnos, T. D. Irons and S. Padilla, Locomotion in larval zebrafish: influence of time of day, lighting and ethanol, *Neurotoxicol.*, 2009, **30**, 52-58.

31. R. M. Basnet, D. Zizioli, S. Taweedet, D. Finazzi and M. Memo, Zebrafish larvae as behavioural model in neuropharmacology, *Biomedicines*, 2019, **7**, 23.

32. L. J. Macaulay, J. M. Bailey, E. D. Levin and H. M. Stapleton, Persisting effects of a pbde metabolite, 6-oh-bde-47, on larval and juvenile zebrafish swimming behavior, *Neurotoxicol. Teratol.*, 2015, **52**, 119-126.

33. C. Y. Usenko, E. M. Robinson, S. Usenko, B. W. Brooks and E. D. Bruce, PBDE developmental effects on embryonic zebrafish, *Environ. Toxicol. Chem.*, 2011, **30(8)**, 1865-1872.

34. S. Ali, D. L. Champagne and M. K. Richardson, Behavioral profiling of zebrafish embryos exposed to a panel of 60 water-soluble compounds. *Behav. Brain Res.*, 2012, **228**, 272-283.

35. S. Ali, D. L. Champagne, A. Alia and M. K. Richardson, Large-scale analysis of acute ethanol exposure in zebrafish development: a critical time window and resilience, *PLoS One*, 2011, **6(5)**, e20037.

36. T. D. Irons, P. E. Kelly, D. L. Hunter, R. C. Macphail and S. Padilla, Acute administration of dopaminergic drugs has differential effects on locomotion in larval zebrafish, *Pharmacol. Biochem. Behav.*, 2013, **103**, 792-813.

37. L. D. Ellis, J. Seibert and K. H. Soanes, Distinct models of induced hyperactivity in zebrafish larvae, *Brain. Res.*, 2012, **1449**, 46-59.

38. A. Binelli, L. Del Giacco, N. Santo, L. Bini, S. Magni, M. Parolini, L. Madaschi, A. Ghilardi, D. Maggioni, M. Ascagni, A. Armini, L. Prosperi, L. Landi, C. La Porta and C. Della Torre, Carbon nanopowder acts as a Trojan-horse for benzo(α)pyrene in *Danio rerio* embryos, *Nanotoxicol.*, 2017, **11(3)**, 371-381.

39. Y. Peng, Y. Luo, X. P. Nie, W. Liao, Y. F. Yang and G. G. Ying, Toxic effects of triclosan on the detoxification system and breeding of Daphnia magna, Ecotoxicol., 2013, **22**, 1384-1394.

40. A. Karami, B. D. Groman, S. P. Wilson, P. Ismail and V. K. Neela, Biomarker responses in zebrafish (*Danio rerio*) larvae exposed to pristine low-density polyethylene fragments, *Environ. Pollut.*, 2017, **223**, 466-475.

41. A. Haegerbaeumer, M-T. Mueller, H. Fueser and W. Traunspurger, Impacts of micro- and nano-sized plastic particles on benthic invertebrates: A literature review and gap analysis, *Front. Environ.*, 2019, **7**, 17.

42. C. C. Parenti, A. Ghilardi, C. Della Torre, M. Mandelli, S. Magni, L. Del Giacco and A. Binelli, Environmental concentrations of triclosan activate cellular defence mechanism and generate cytotoxicity on zebrafish (*Danio rerio*) embryos, Sci. Tot. Environ., 2019, **650**, 1752-1758.

43. H. Bloemendal, W. De Jong, R. Jaenicke, N. H. Lubsen, C. Slingsby and A. Tardieu, Ageing and vision: Structure, stability and function of lens crystallins, *Prog. Biophys. Mol. Biol.*, 2004, **86**, 407-485.

44. Y. R. Lin, H. K. Mok, Y. H. Wu, S. S. Liang, C. C. Hsiao, C. H. Huang and S. H. Chiou, Comparative proteomics analysis of degenerative eye lenses of nocturnal rice eel and catfish as compared to diurnal zebrafish, *Mol. Vision*, 2013, **19**, 623-637.

45. A. Pande, J. Pande, N. Asherie, A. Lomakin, O. Ogun, J. King and G. B. Benedek, Crystal cataracts: Human genetic cataract caused by protein crystallization, *PNAS*, 2001, **98(11)**, 6116-6120.

46. A. Mumford, I. Cree, J. Arnold, M. Hagan, K. Rixon and J. Harding, The lens in hereditary hyperferritinaemia cataract syndrome contains crystalline deposits of L-ferritin, *Br. J. Ophthalmol.*, 2000, **84**, 697-700.

47. H. L. Bader, E. Lambert, A. Guiraud, M. Malbouyres, W. Driever, M. Koch and F. Ruggiero, Zebrafish collagen XIV is transiently expressed in epithelia and is required for proper function of certain basement membranes, *J. Biol. Chem.*, 2013, **288**, 6777-6787.

48. T. Manon-Jensen and M. A. Karsdal, in *Biochemistry of collagens, laminins and elastin: Structure, function and biomarkers*, ed. M. A. Karsdal, ScienceDirect, 272, 2016.

49. J-B. Oudart, J-C. Monboisse, F. X. Maquart, Type XIX collagen: A new partner in the interactions between tumor cells and their microenvironment, *Matrix Biol.*, 2017, **57-58**, 169-177.

50. B. B. Young, G. Zhang, M. Koch and D. E. Birk, The roles of types XII and XIV collagen in fibrillogenesis and matrix assembly in the developing cornea, *J. Cell. Biochem.*, 2002, **87**, 208-220.

51. M. van Pomeren, N. R. Brun, W. J. G. M. Peijnenburg and M. G. Vijver, Exploring uptake and biodistribution of polystyrene (nano)particles in zebrafish embryos at different developmental stages, *Aq. Toxicol.*, 2017, **190**, 40-45.

52. W. S. Lee, H-J. Cho, E. Kim, J. H. Hu, H-J. Kim, B. Kim, J-S., Lee and J. Jeong, Bioaccumulation of polystyrene nanoplastics and their effect on the toxicity of Au ions in zebrafish embryos, *Nanoscale*, 2019, **11**, 3173.

53. S. A. M. Martin, O. Vilhelmsson, F. Médale, P. Watt, S. Kaushik and D. F. Houlihan, Proteomic sensitivity to dietary manipulations in rainbow trout, *Biochim. Biophys.*, 2003, **1651**, 17-29.

54. O. T. Vilhelmsson, S. A. M. Martin, F. Mèdale, S. J. Kaushik and D. F. Houli-han, Dietary plant-protein substitution affects hepatic metabolism in rainbow trout (*Oncorhynchus mykiss*), *Br. J. Nutr.*, 2004, **92**, 71-80.

55. R. W. Smith, P. Cash, S. Ellefsen and G. E. Nilsson, Proteomic changes in the crucian carp brain during exposure to anoxia, *Proteomics*, 2009, **9**, 2217-2229.

56. P. Gómez-Requeni, L. E. C. Conceição, A-E. Olderbakk Jordal and I. Rønnestad, A reference growth curve for nutritional experiments in zebrafish (*Danio rerio*) and changes in whole body proteome during development, *Fish Physiol. Biochem.*, 2010, **36**, 1199-1215.

57. Rao, K.S., Albro, M., Dwyer, T.M., Frerman, F.E. 2006. Kinetic Mechanism of Glutaryl-CoA Dehydrogenase. Biochemistry, 45-51, 15853-15861.

58. J. Gao, C. Zhang and X. Luo, Effects of targeted suppression of glutaryl-CoA dehydrogenase by lentivirus-mediated shRNA and excessive intake of lysine on apoptosis in rat striatal neurons, *PLoS One*, 2013, **8(5)**, e63084.

59. T-H. Shih, J-L. Horng, P-P. Hwang and L-Y. Lin, Ammonia excretion by the skin of zebrafish (*Danio rerio*) larvae, *Am. J. Physiol. Cell. Physiol.*, 2008, **295**, 1625-1632.

60. M. Codina, J. Li, J. Gutiérrez, J. P. Y. Kao and S. J. Du, Loss of Smyhc1 or Hsp90alpha1 function results in different effects on myofibril organization in skeletal muscles of zebrafish embryos, *PLoS One*, 2010, **5**, e8416.

61. H. Nord, A. C. Burguiere, J. Muck, C. Nord, U. Ahlgren and J. von Hofsten, Differential regulation of myosin heavy chains defines new muscle domains in zebrafish, *Mol. Biol. Cell.*, 2014, **25**, 1384-1395.

62. J. B. Buhrdel, S. Hirth, M. Kessler, S. Westphal, M. Forster, L. Manta, G. Wiche, B. Schoser, J. Schessl, R. Schroder, C. S. Clemen, L. Eichinger, D. O. Furst, P. F. van der Ven, W. Rottbauer and S. Just, In vivo characterization of human myofibrillar myopathy genes in zebrafish, *Biochem. Biophys. Res. Commun.*, 2015, **461**, 217-223.

63. K. Henke, J. M. Daane, M. B. Hawkins, C. M. Dooley, E. M. Busch-Nentwich, D. L. Stemple and M. P. Harris, Genetic screen for postembryonic development in the zebrafish (*Danio rerio*): Dominant mutations affecting adult form, *Genetics*, 2017, **207**, 609-623.

64. G. Asmonaite, H. Sundh, N. Asker and B. C. Almroth, Rainbow trout maintain intestinal transport and barrier functions following exposure to polystyrene microplastics, *Environ. Sci. Technol.*, 2018, **52**, 14392-14401.

65. J. Hou, in *The Paracellular Channel: Biology, Physiology and Disease*, Elsevier, 248, 2019.

66. C. T. Capaldo and A. Nusrat, Claudin switching: Physiological plasticity of the tight junction, *Semin. Cell. Dev. Biol.*, 2015, **42**, 22-29.

67. A. Tervonen, T. O. Ihalainen, S. Nymark and J. Hyttinen, Structural dynamics of tight junctions modulate the properties of the epithelial barrier, *PLoS One*, 2019, 0214876.

68. C. M. Van Itallie, J. Holmes, A. Bridges and J. M. Anderson, Claudin-2-dependent changes in noncharged solute flux are mediated by the extracellular domains and require attachment to the PDZ-scaffold, *Ann. N. Y. Acad. Sci.*, 2009, **1165**, 82-87.

69. M. M. Buschmann, L. Shen, H. Rajapakse, D. R. Raleigh, Y. Wang, Y. Wang, A. Lingaraju, J. Zha, E. Abbott, E. M. McAuley, L. A. Breskin, L. Wu, K. Andreson, J. R. Turner and C. R. Weber, Occludin OCEL-domain interactions are required for maintenance and regulation of the tight junction barrier to macromolecular flux, *Mol. Biol. Cell.*, 2013, **24**, 3056-3068.

70. C. Riva, S. Cristoni and A. Binelli, Effects of triclosan in the freshwater *Dreissena polymorpha*: A proteomic investigation, *Aquat. Toxicol.*, 2012, **118-119**, 62-71.

71. C. Wilson and C. Gonzalez-Billault, Regulation of cytoskeletal dynamics by redox signaling and oxidative stress: Implications for neuronal development and trafficking, *Front. Cell. Neurosci.*, 2015, **9**, 381.

72. E. Belcastro, W. Wu, I. Fries-Raeth, A. Corti, A. Pompella, P. Leroy, I. Larteaud and C. Gaucher, Oxidative stress enhances and modulates protein S-nitrosation in smooth muscle cells exposed to S-nitrosoglutathione, *Nitric Oxide*, 2017, **69**, 10-21.

Table 1. Concentrations of PNPs and TCS used for the preparation of TCS-contaminated particles suspension.

	Preparation solutions		Final concentration of solution	Exposure concentrations
	Stock solution	*Working solution*	*Extract*	
PNPs	100 g/L	2.5 g/L	-	200 µg/L
TCS	1 mg/L	250 µg/L	82 µg/L	0.6 µg/L

View Article Online
DOI: 10.1039/D0EN00961J

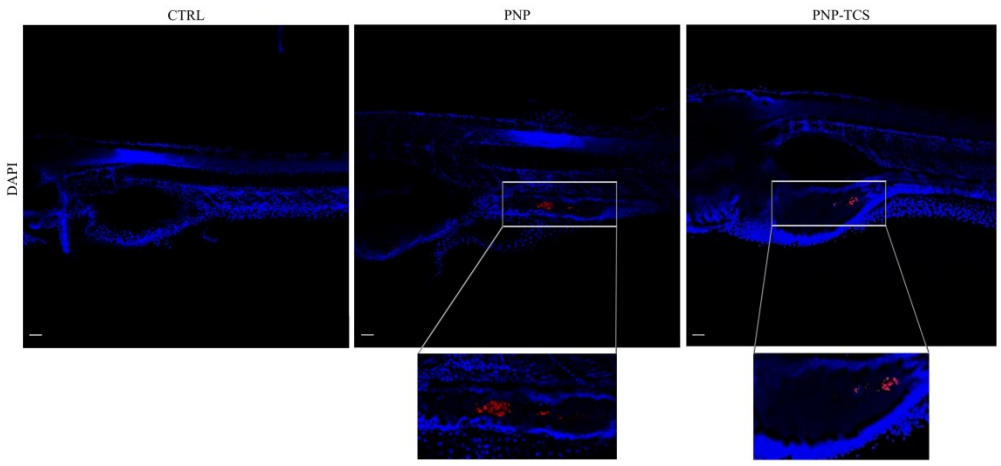

Fig.1. Whole mount images of larvae at the end of the exposure (scale bar 50 μm). Nanobeads are shown in red. Cell nuclei are stained with DAPI.

253x123mm (300 x 300 DPI)

View Article Online
DOI: 10.1039/D0EN00961J

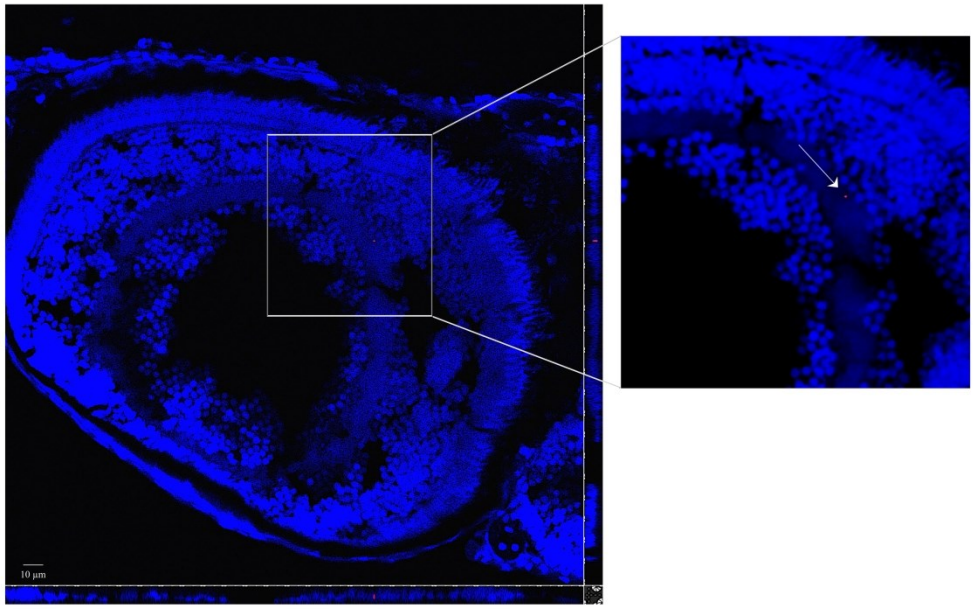

Fig.2. Detail of a cryostate section (11 Z-step of 1 µm) showing the eye of a zebrafish larva exposed to PNP-TCS. Nanobeads are shown in red. Cell nuclei are stained with DAPI. Orthogonal projections of Z-stack evidencing the nanobead at cellular level.

249x157mm (300 x 300 DPI)

View Article Online
DOI: 10.1039/D0EN00961J

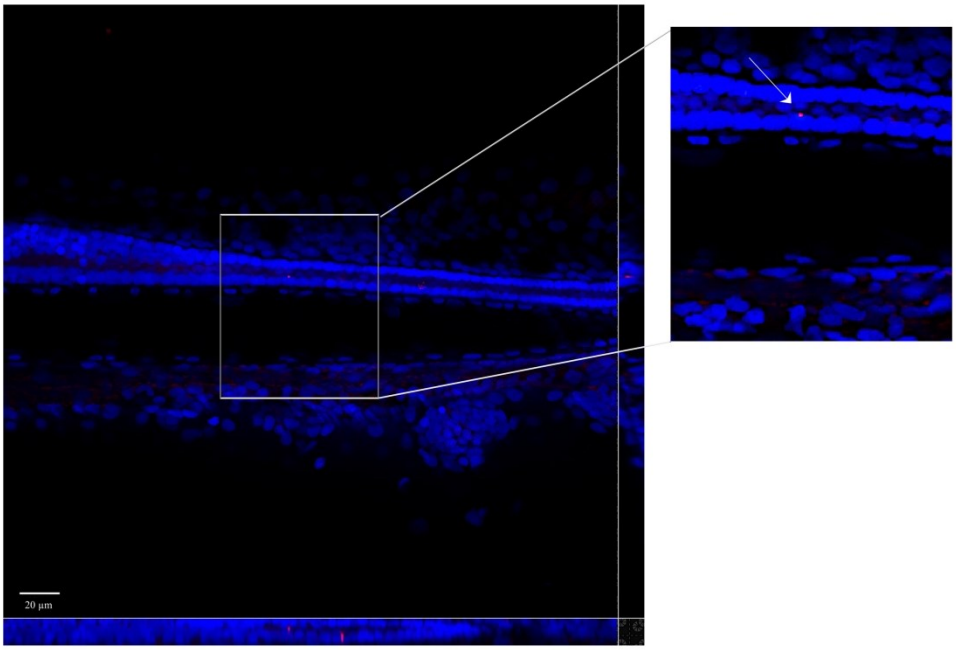

Fig.3. Detail of a cryostate section (14 Z-step of 1 µm) showing the tail of a zebrafish larva exposed to PNP. Nanobeads are shown in red. Cell nuclei are stained with DAPI. Orthogonal projections of Z-stacks evidencing the nanobead at cellular level.

232x158mm (300 x 300 DPI)

View Article Online
DOI: 10.1039/D0EN00961J

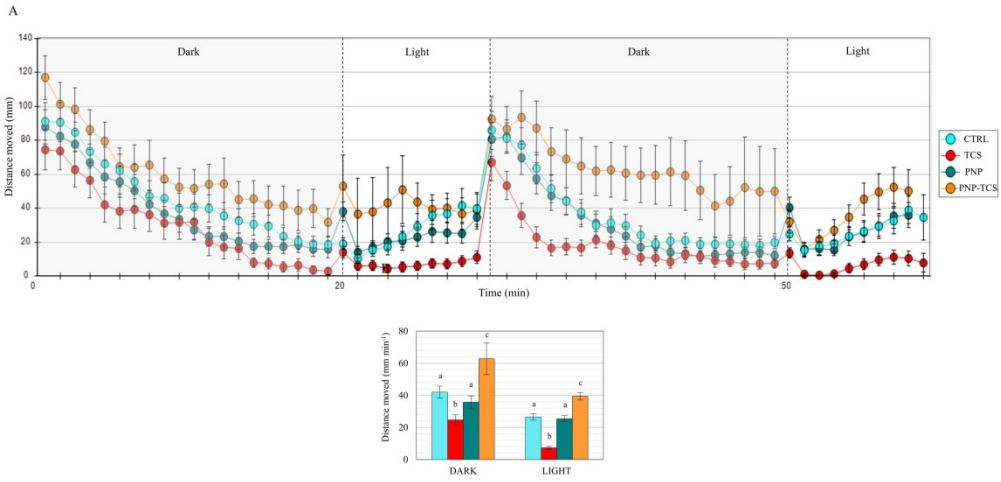

Fig.4. Swimming activity (distance moved over time) measured in zebrafish larvae exposed to PNP (200 µg/L), TCS (0.6 µg/L) and PNP-TCS, compared to control. (A) Total distance moved per minute (mean±S.E.); (B) Total distance moved during dark and light conditions (mean±S.E.). Different letters correspond to values significantly different (one-way ANOVA and DMRT post-hoc test, $p<0.05$).

253x127mm (300 x 300 DPI)

View Article Online
DOI: 10.1039/D0EN00961J

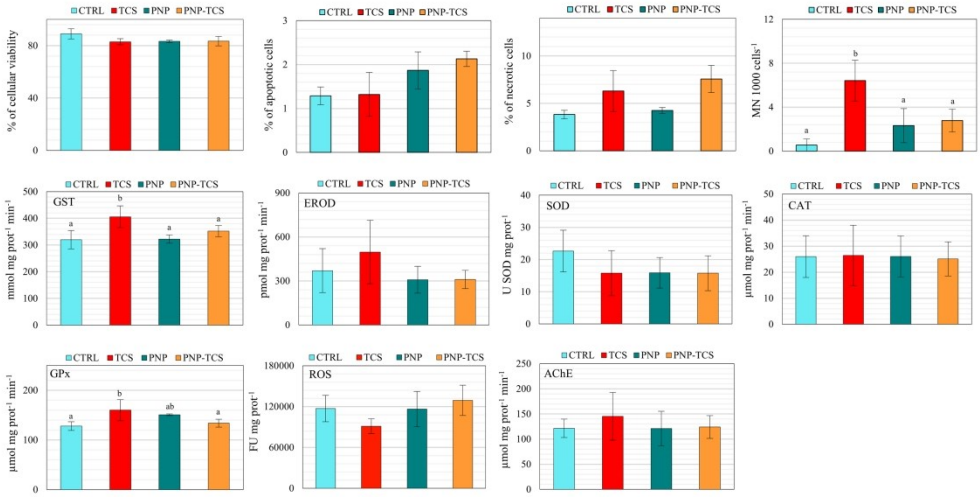

Fig.5. Cellular effects measured in zebrafish larvae exposed to PNP (200 µg/L), TCS (0.6 µg/L) and PNP-TCS, compared to control (pool of 3 independent experiments). Different letters correspond to values significantly different (one-way ANOVA and DMRT post-hoc test, $p<0.05$).

243x130mm (300 x 300 DPI)

View Article Online
DOI: 10.1039/D0EN00961J

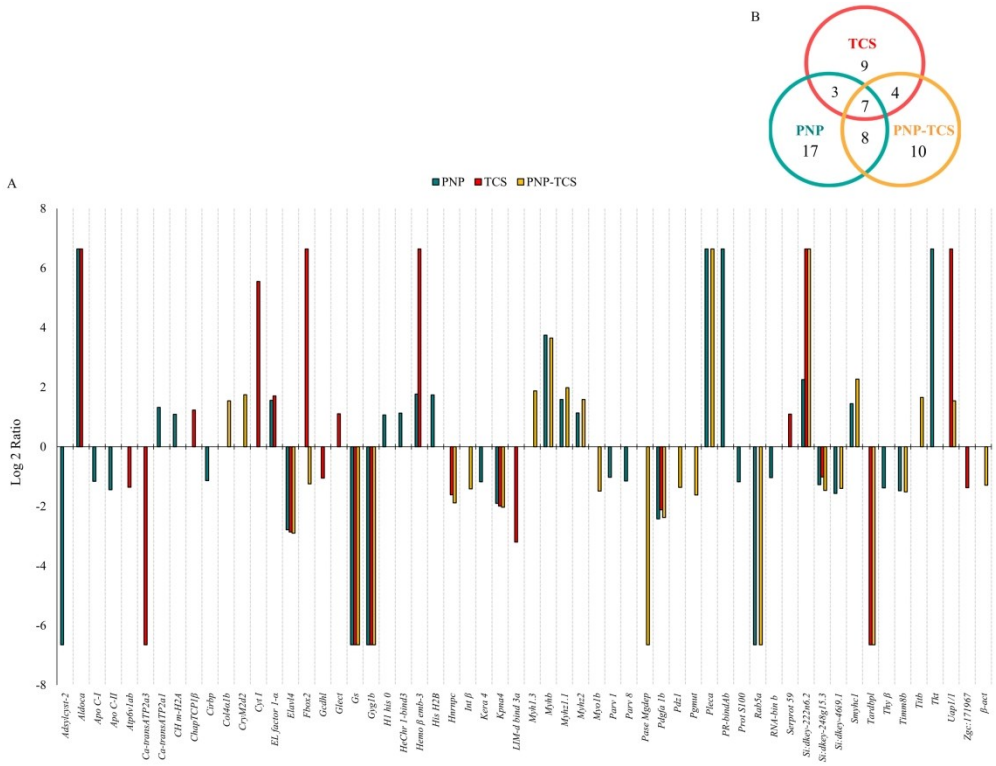

Fig.6. (A) Protein modulation measured in zebrafish larvae exposed to PNP (200 µg/L), TCS (0.6 µg/L) and PNP-TCS, compared to control; (B) Venn diagram. Adsylcyst-2: s-adenosylhomocysteine hydrolase-like 2; Aldoca: fructose-bisphosphate aldolase; Apo C-I: apolipoprotein c-i; Apo C-II: apolipoprotein c-ii; Atp6v1ab: atpase h+-transporting v1 subunit ab; Ca-transATP2a3: calcium-transporting atpase GN=atp2a3; Ca-transATP2a1: calcium-transporting atpase GN=atp2a1; CH m-H2A: core histone macro-h2a; ChapTCP1β: chaperonin containing tcp1, subunit 2 (beta); Cirbp: cirbp protein; Col4α1b: collagen, type xiv, alpha 1b; CryM2d2: crystallin, gamma m2d2; Cyt I: type i cytokeratin; EL factor 1-α: elongation factor 1-alpha; Elavl4: elav-like protein; Fbxo2: f-box protein 2; Gcdhl: glutaryl-coa dehydrogenase b; Glect: galectin; Gs: glutamine synthetase; Gyg1b: glycogenin 1b; H1 his 0: h1 histone family, member 0; HeChr 1-bind3: heterochromatin protein 1, -binding protein 3; Hemo β emb-3: hemoglobin beta embryonic-3; His H2B: histone h2b; Hnrnpc: heterogeneous nuclear ribonucleoprotein c1/c2; Int β: integrin beta; Kera 4: keratin 4; Kpna4: importin subunit α; LIM-d bind 3a: lim-domain binding factor 3a; Myh1.3: myosin, heavy polypeptide 1.3, skeletal muscle; Myhb: myosin, heavy chain b; Myhz1.1: myosin, heavy polypeptide 1, skeletal muscle; Myhz2: myosin, heavy polypeptide 2, fast muscle-specific; Myo1b: myozenin 1b; Parv 1: parvalbumin 1; Parv 8: parvalbumin 8; Pase Mgdep: protein phosphatase, mg2+/mn2+-dependent, 1aa; Pdgfa 1b: pdgfa associated protein 1b; Pdz1: pdz domain-containing 1; Pgmut: phosphoglycerate mutase; Pleca: plectin a; PR-bindAb: purine-rich element-binding protein ab; Prot S100: protein s100; Rab5a: rab5a protein; RNA-bin b: cold-inducible rna-binding protein b; Serprot 59: serine protease 59, tandem duplicate 2; Smyhc1: slow myosin heavy chain 1; Tardbpl: tar dna-binding protein, -like; Thy β: thymosin beta; Timm8b: translocase of inner mitochondrial membrane 8 homolog b; Titb: titin b; Tkt: tkt protein; Uap1/1: udp-n-acetylhexosamine pyrophosphorylase-like protein 1; β-act: beta-actin.

251x192mm (300 x 300 DPI)

View Article Online
DOI: 10.1039/D0EN00961J

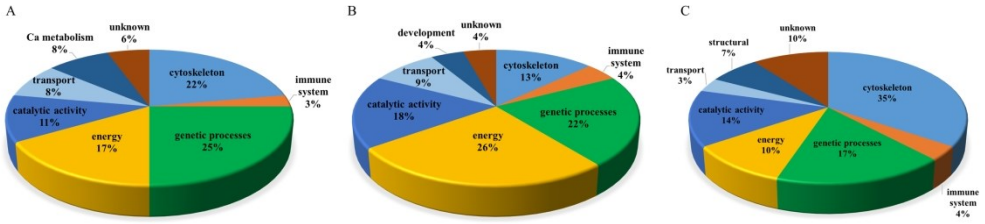

Fig.7. Molecular functions of modified proteins in zebrafish larvae exposed to (A) PNP (200 μg/L), (B) TCS (0.6 μg/L) and (C) PNP-TCS.

250x62mm (300 x 300 DPI)

View Article Online
DOI: 10.1039/D0EN00961J

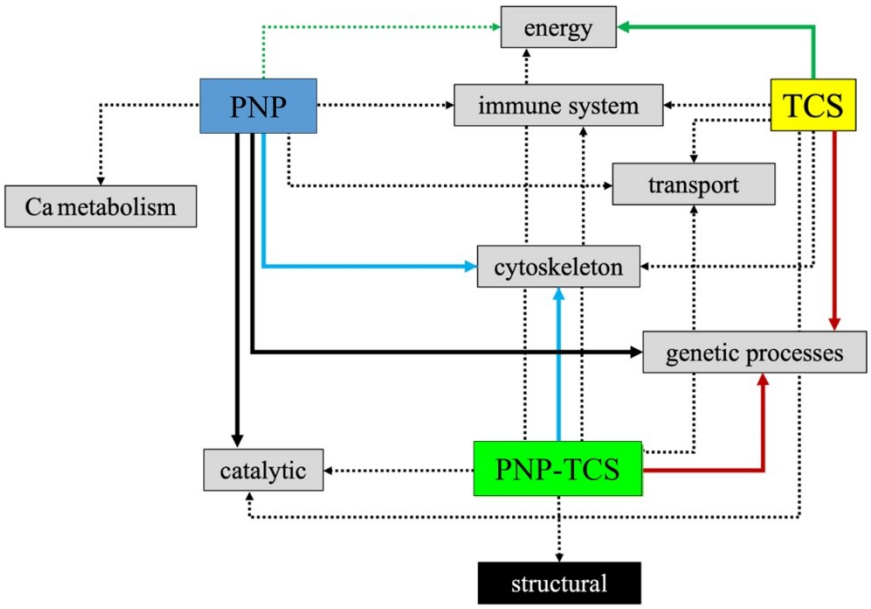

Fig.8. Outline of proteomic results: dotted lines=low to medium effect of the contaminant; solid lines=high effect of the contaminant; same colour=similar effect of contaminants (high number of co-modulated proteins).

157x108mm (300 x 300 DPI)

View Article Online
DOI: 10.1039/D0EN00961J

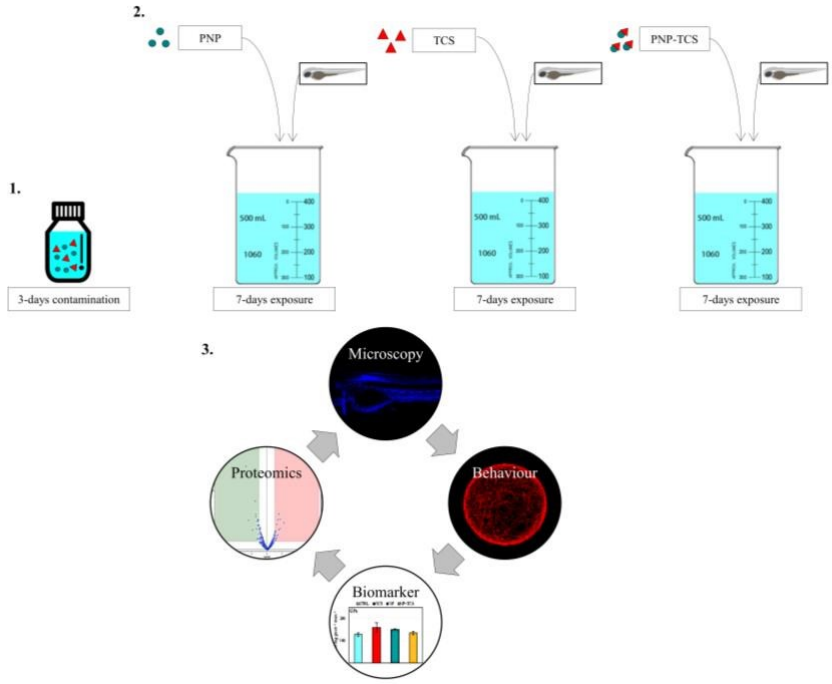

The risk associated to the action of nanoplastics as carrier of environmental pollutants investigated by a multi-tiered approach.